

# Superstructure Optimization of International Hydrogen Supply Chain with Technological Options

Juyeong Jung\* Jay H. Lee\*\* Wonsuk Chung\*\*\* Seongmin Heo\*

\* Department of Chemical and Biomolecular Engineering, Korea Advanced Institute of Science and Technology (KAIST), Daejeon, Korea (e-mail: [smheo@kaist.ac.kr](mailto:smheo@kaist.ac.kr))

\*\* Department of Chemical and Materials Science and of Aerospace and Mechanical Engineering, University of Southern California, Los Angeles, CA 90007 USA (e-mail: [jlee4140@usc.edu](mailto:jlee4140@usc.edu))

\*\*\* Clean Energy Research Center, Korea Institute of Science and Technology (KIST), 02792 Seoul, Korea

---

**Abstract:** In the pursuit of reducing carbon emissions, the integration of renewable energy into society's energy portfolio plays a crucial role despite challenges tied to their inherent unpredictability and seasonal variations. Hydrogen, as a mean of storing and transporting renewable energy becomes crucial in addressing these challenges. Notwithstanding its potential, the misalignment of cost-competitive hydrogen production hubs with demand centers calls for a thorough examination of global hydrogen distribution. The versatility of hydrogen transportation (e.g., pipelines, ships, trucks) and various forms like compressed hydrogen, liquid hydrogen, ammonia, and liquid organic hydrogen carriers (LOHC) adds complexity to designing an economically efficient hydrogen supply chain (HSC). Addressing previous scholarly limitations focused on existing technologies, this study advocates for a superstructure-based modeling approach for HSC that includes promising technologies. Through a case study involving a production site in the Middle East and a demand site in Texas, a dedicated HSC superstructure network is formulated, facilitating the identification of cost-effective hydrogen supply pathways using Mixed Integer Linear Programming. Ultimately, this effort aims to establish a comprehensive framework to discern the most sustainable and financially viable technologies, identifying the optimal configuration within the HSC.

**Keywords:** Hydrogen supply chain, Process modeling, Superstructure optimization, Mixed Integer Linear Programming

---

## 1. INTRODUCTION

Renewable energy, particularly sourced from solar and wind, is anticipated to play a pivotal role in decarbonization. However, the unpredictability and seasonal variations inherent to renewable resources pose challenges to their seamless integration into the energy portfolio. In response, hydrogen emerges as a vital energy carrier for storing and transporting energy derived from renewables, owing to its notably high energy density, approximately three times that of diesel fuel (Nicoletti et al., 2015).

Hydrogen is produced from diverse resources such as renewable electricity, nuclear, natural gas, biogas, coal, and industrial off-gas (Kalamaras & Efstathiou, 2013). Despite its potential, cost-competitive hydrogen production hubs are located far from demand centers. Therefore, a comprehensive analysis of the international distribution of hydrogen, a substantial aspect of the overall hydrogen supply chain (HSC), is essential for estimating hydrogen costs along the supply chain. Furthermore, hydrogen can be transported with various transportation modalities, including pipelines, ships, and trucks, and also in various forms, such as compressed hydrogen, liquefied hydrogen, ammonia, and liquid organic hydrogen carriers (LOHC) (Hurskainen & Itonen, 2020; Noh et al., 2023). While numerous technologies related to hydrogen production and distribution exist, cost-effective HSC designs

still remain elusive. Geographical considerations, diverse energy sources, and varied transportation options contribute to the complexity of designing an optimal HSC.

A large number of studies have been conducted on the design and operation of HSCs in various geographical contexts. Agnolucci and McDowall classified the HSC model into three types: energy system optimization, geographically explicit optimization, and refueling station locating models (Agnolucci & McDowall, 2013). Specifically, the energy system optimization model has been employed to identify hydrogen-based energy systems with minimal cost using LP/MILP (Endo, 2007; Gül et al., 2009; Rosenberg et al., 2010; Strachan et al., 2009). In addition, the geographically explicit optimization model generally encompasses the entire HSC at a national or regional scale and thus is utilized in the deployment of infrastructures. Specifically, binary and integer decision variables are used in a geographical optimization model to enable the optimal selection of transportation modes, location of facilities, sizing decisions, and suitable technologies (Almansoori & Shah, 2006; Eskandarpour et al., 2015; Tsuda et al., 2014). For the refueling station-locating model type, a number of developed models have been implemented to optimize a network of hydrogen refueling stations at an urban scale (Kuby et al., 2009; Kuby & Lim, 2005; Lin et al., 2008). Additionally, a significant portion of

research on designing HSCs has primarily concentrated on hydrogen as the exclusive energy carrier to fulfill consumer needs, specifically in meeting transportation demands entirely. Previous modeling efforts aimed at HSCs primarily focused on analyzing their design without considering systems incorporating various energy sources and multiple transportation modes. Furthermore, these approaches do not address both existing and promising technologies, limiting their capacity to incorporate transitions from existing infrastructure.

Motivated by these limitations, in this work, a superstructure-based modeling of hydrogen production and distribution system is proposed to consider the promising technologies of HSC in addition to conventional technologies. Modeling of early-stage technologies of HSC (e.g., H<sub>2</sub> to LOHC conversion process) is performed for which commercial data are unavailable. Furthermore, the sources, demand, and production sites are designated for a case study involving targeted geographical areas (i.e., Saudi Arabia and the United States), and a specific HSC superstructure network is constructed for it. Subsequently, a set of scenarios is created by specifying utility supply and the prospect of market demand. Lastly, the cost-efficient hydrogen supply pathways within the constructed superstructure network are identified using Mixed Integer Linear Programming. Notably, this proposed work develops the framework and methodology for simultaneously identifying the cost-efficient configuration of the HSC through superstructure modeling, numerical evaluation, and optimization.

## 2. SYSTEM DESCRIPTION

### 2.1 Hydrogen supply chain superstructure

The primary objective of constructing the superstructure model is to facilitate the selection of optimal combination within the HSC. Therefore, it is imperative to compile available options for each entity, creating a network that represents the HSC. The network combines essential steps, resulting in various cases that depict potential processing paths from feedstocks to end applications, such as mobility, energy sources, or chemical production. Accordingly, this work presents a comprehensive HSC superstructure model encompassing available options for raw material and energy sourcing, manufacturing, storage, and transportation phases essential for hydrogen production and distribution (Fig. 1).

The HSC superstructure network, in this study, incorporates six feedstocks for hydrogen production, five main production methods, four hydrogen state options for transport, eight transportation alternatives, and four reconversion methods. Supplying hydrogen as an energy carrier initiates with various feedstocks, including natural gas, coal, biomass, nuclear, wind and solar energies. Depending on each energy source, hydrogen is produced by steam reforming, coal gasification, biomass gasification, or water electrolysis. Subsequently, the produced hydrogen undergoes conditioning, resulting in compressed hydrogen, liquid hydrogen, ammonia, or liquid organic hydrogen carrier (LOHC). These conditioned forms are transported via shipping from the production site to the demand site, then are delivered to the appropriate storage and

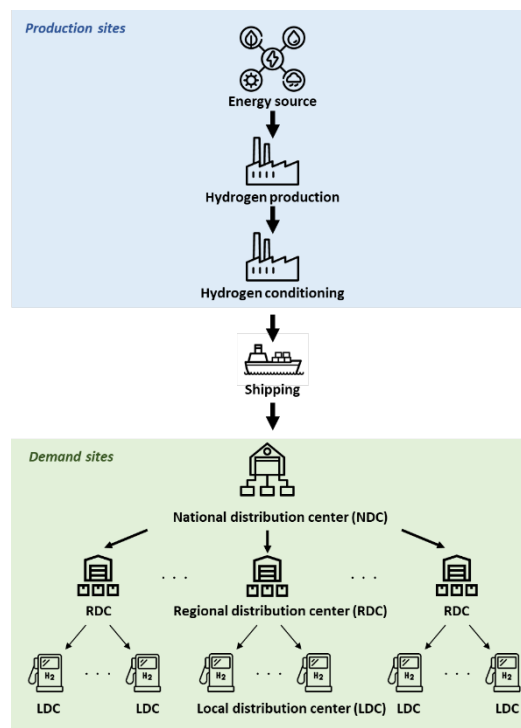


Figure 1. Schematic illustration of hydrogen supply chain system

transportation modes before being reconverted at a refueling station to supply the end product to consumers.

### 2.2 Distribution system

The distribution system in the demand site, in this work, is structured as a three-echelon mirroring real logistics (Fig. 1). An external supplier from a production site, handling the hydrogen production and conditioning facilities at the same locations, provides hydrogen to the National Distribution Center (NDC). The NDC serves as a hub, consolidating shipments from international manufacturers and dispatching them to Regional Distribution Centers (RDCs). Regional transportation modes then convey the hydrogen from the NDC to RDCs, crucial for consolidating shipments and mitigating risks. At the base level, a Local Distribution Center (LDC) functions as a refueling station, meeting the demands of end customers.

### 2.3 Transportation system

In this work, the hydrogen transportation system within the supply chain encompasses both intermodal and multimodal services. Intermodality refers to a method of hydrogen transportation where different transportation modes are interconnected to form a seamless network, ensuring efficient coordination between various components. Accordingly, the delivery for energy source, shipping, NDC to RDCs, and RDCs to LDCs are all included in the HSC superstructure.

Multimodality involves utilizing two or more transportation modes in parallel. Thus, in this work, hydrogen transport with diverse conditions employs with trailers, railways, pipelines between NDC to RDCs, and trailers, pipelines between RDCs to LDCs.

### 3. DATABASE CONSTRUCTION

#### 3.1 Database construction for transportation system

The hydrogen transportation system is divided into regional and local components. The regional system addresses intercity distribution, utilizing Geographic Information System (GIS) data. Fig. 2 exemplifies regional transportation, featuring the railway system. In this work, distances of regional modes (i.e., railway, pipeline, and roads) are derived using the ArcGIS program. For instance, the shortest distance of railway from Houston to Dallas, which is the regional transportation system, is depicted as red line in Fig. 2.



Figure 2. Texas railway system from ArcGIS

A comprehensive elucidation of local transportation systems requires the ability to depict the deployment of refueling stations. This aspect exhibits significant variability across cities, thereby necessitating the development of a universal model capable of accommodating diverse urban contexts. To address this imperative, in this work, the Idealized Refueling Station Network Model is adopted (Fig. 3) (Yang & Ogden, 2007). The model is grounded in several assumptions: 1. the homogeneous distribution of the population within a circular city, 2. the arrangement of refueling stations in concentric rings around the city center, and 3. uniform station capacity. Using these assumptions, the distances for local transportation modes, such as pipelines, trucks (i.e., trailers) are calculated using (1) and (2).

$$LDiS_{trailer} = 1.44 \cdot r_{city} \cdot N_{stations} \quad (1)$$

$$LDiS_{pipeline} = 2.43 \cdot r_{city} \cdot N_{stations}^{0.4909} \quad (2)$$

Here,  $r_{city}$  is the radius of a city, and  $N_{stations}$  is the number of stations in a city.

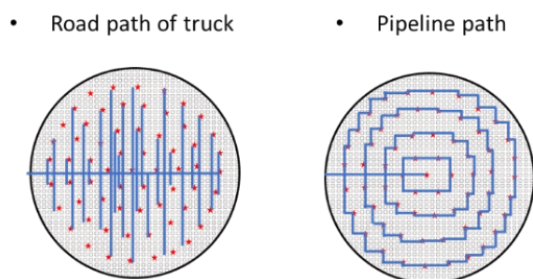


Figure 3. Road & Pipeline path model based on Idealized Refueling Station Network Model

#### 3.2 Process simulation for early-stage technology data

To comprehensively explore all identified potential technologies within the HSC design, early-stage technologies like LOHC conditioning and dehydrogenation are also incorporated into the superstructure. Given the absence of data for the processes in existing literature or commercial sources, in this work, process modeling and evaluation are undertaken. Specifically, ammonia production, ammonia cracking, formic acid (FA) conditioning, and FA dehydrogenation processes are simulated using Aspen Plus.

As a technology option of LOHC in conditioning part, in this work, the formic acid is adopted due to its biodegradable characteristic, low flammability, and stability under ambient conditions. Notably, the conditioning to FA is achieved through CO<sub>2</sub> hydrogenation, diverging from conventional production methods. While conventional FA production involves carbon monoxide and steam as raw materials, which do not involve hydrogen, the CO<sub>2</sub> hydrogenation process is chosen as a conditioning option for converting hydrogen to FA. In this regard, Triethylamine and N-butylimidazole-based CO<sub>2</sub> hydrogenation process, an early-stage technology, is employed, utilizing CO<sub>2</sub> and H<sub>2</sub> as raw materials. The simulation results of CO<sub>2</sub> hydrogenation FA production are presented in Table 1. Subsequently, a techno-economic analysis is conducted to extract necessary data (i.e., capital cost, operating cost) by utilizing the mass and energy balance obtained from each process simulation.

Table 1. Mass and energy balance of CO<sub>2</sub> hydrogenation formic acid production from the simulation results

		Total incident flow	Unit
<b>Raw material</b>	Natural Gas	0.102	ton/ton FA
	CO <sub>2</sub>	0.42	ton/ton FA
	Triethylamine	0.00047	ton/ton FA
	N-butylimidazole	0.00057	ton/ton FA
<b>Utility</b>	Heat- MP steam	17.730	GJ/ton FA
	Heat- NG combustion	0.023	ton/ton FA
	Electricity mix	0.954	GJ/ton FA
<b>Direct emission</b>	CO <sub>2</sub>	0.061	ton/ton FA

### 4. OPTIMIZATION FORMULATION

Using the compiled database, which includes technical data from the literature, process simulation data, cost parameter, and spatial information, the optimization model encompasses the mass/energy balance, cost calculation and demand estimation with market penetration rates as elucidated in Fig. 4. The objective of the optimization is to minimize the total

daily cost of the entire HSC. The decision variables in the proposed HSC include the number of hydrogen facilities and their capacities, transportation connections, the number of transportation vehicles, and hydrogen flow distribution within the superstructure network. Formulated as a mixed-integer linear programming (MILP) problem, the model is solved using the CPLEX solver within the *Pyomo* environment. Subsequently, the results provide the optimal configuration, the levelized hydrogen cost of the whole supply chain, and the associated decision variables.

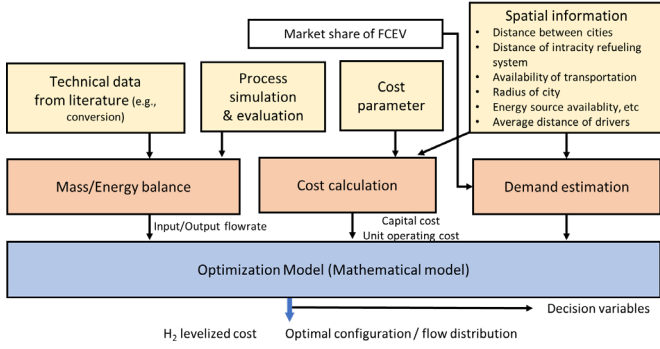


Figure 4. Optimization formulation for cost-efficient hydrogen supply chain

#### 4.1 Objective function

The total daily cost of the HSC is given as in

$$\begin{aligned} \text{Total daily cost} = & ESC + PC + CC + ShipC + RTC \\ & + LTC + SC + RC \end{aligned} \quad (3)$$

Here,  $ESC$  is the energy source cost,  $PC$  is the hydrogen production cost,  $CC$  is the conditioning cost,  $ShipC$  is the shipping cost,  $RTC$  is the regional transportation cost,  $LTC$  is the local transportation cost,  $SC$  is the hydrogen storage cost, and  $RC$  is the reconversion to hydrogen cost. Each cost component is calculated as follows:

$$ESC = \sum_e \left( \sum_p f_{e,p}^E \right) (ESDelivery_e \cdot ESDis_e + ESP_e) \quad (4)$$

In the above,  $ESDelivery_e$  denotes the delivery cost of energy source  $e$ ,  $ESDis_e$  represents the distance between resource  $e$  and hydrogen production locations,  $ESP_e$  is the price of energy source  $e$ .

The cost calculation related to the hydrogen process are represented as follows:

$$PC = \sum_p (CRF_p \times (PCC_p \times NP_p) + Pr_p \times POC_p) \quad (5)$$

$$CC = \sum_c (CRF_c \times (CCC_c \times NC_c) + Cr_c \times COC_c) \quad (6)$$

$$SC = \sum_{s,c} (CRF_s \times (SCC_s \times NS_s) + SInv_s \times SOC_s) \quad (7)$$

$$RC = \sum_r (CRF_r \times (RCC_r \times NR_r) + Rr_r \times ROC_r) \quad (8)$$

In the above,  $PCC_p$ ,  $CCC_c$ ,  $SCC_s$ , and  $RCC_r$  indicate the capital costs of hydrogen production, conditioning, storage, and reconversion, respectively,  $POC_p$ ,  $COC_c$ ,  $SOC_s$ , and  $ROC_r$  denote the operating costs of hydrogen production  $p$ , conditioning  $c$ , storage  $s$ , and reconversion  $r$ , respectively,  $CRF_p$ ,  $CRF_c$ ,  $CRF_s$ , and  $CRF_r$  are the capital recovery factors (CRF) of hydrogen production, conditioning, storage, and reconversion, respectively. Each cost calculation is conducted based on both the number of facilities ( $NP_p$ ,  $NC_c$ ,  $NS_s$ , and  $NR_r$ ) and throughputs ( $Pr_p$ ,  $Cr_c$ ,  $SInv_s$ , and  $Rr_r$ ).

To incorporate international hydrogen trade, the shipping cost from the production site to the demand site is included in the total HSC cost as shown below:

$$ShipC = \sum_c (Cr_c \cdot (2 \times IntDIS) \cdot UShipC_c) \quad (7)$$

where  $IntDIS$  is the international shipping distance from the production site to the demand site, and  $UShipC_c$  is the unit shipping cost of condition  $c$  per distance under the unit capacity.

The costs for the regional and local transportation systems are calculated as the sum of the operating cost (i.e., fuel cost, labor cost, maintenance cost) and the capital cost of a transportation mode, as follows:

$$\begin{aligned} RTC = \sum_t ((CRF_t \times RTCC_t \times NRT_t) \\ + RFC + RLC + RMC) \end{aligned} \quad (9)$$

$$\begin{aligned} LTC = \sum_l ((CRF_l \times LTCC_l \times NLT_l) \\ + LFC + LLC + LMC) \end{aligned} \quad (10)$$

where  $CRF_t$  and  $CRF_l$  are the CRF of regional and local transport, respectively.  $RTCC_t$  and  $LTCC_l$  are the capital costs of regional ( $t$ ) and local ( $l$ ) transport modes, respectively.  $RFC$  and  $LFC$  are the fuel cost, while  $RLC$  and  $LLC$  are the labor cost. Additionally,  $RMC$  and  $LMC$  are the maintenance cost of regional and local transport modes, respectively.

#### 4.2 Constraints

The demand for energy source must be satisfied to ensure production throughput, as indicated in (11) and (12). Hydrogen production is executed by employing each production technology  $p$  with specified energy sources  $e$ . The production rate, conditioning rate, and reconversion rate are determined by considering both the flow rates from the previous step and a predetermined conversion ratio corresponding to the technology, as follows:

$$ED_e = \sum_p f_{e,p}^E \quad (11)$$

$$Pr_p = \left( \sum_e f_{e,p}^E \right) \cdot Pconv_p \quad (12)$$

$$Cr_c = \left( \sum_p f_{p,c}^P \right) \cdot Cconv_c \quad (13)$$

$$Rr_r = \left( \sum_{s_3} f_{s_3,r}^{S_3} \right) \cdot Rconv_r \quad (14)$$

where  $f_{e,p}^E$  is the flowrate from the energy source ( $e$ ) to the production part ( $p$ ),  $f_{p,c}^P$  is the flowrate from the production part ( $p$ ) to the conditioning part ( $c$ ), and  $Pconv_p$ ,  $Cconv_c$ , and  $Rconv_r$  are the conversion ratios for the production ( $p$ ), conditioning ( $c$ ), and reconversion ( $r$ ), respectively.

The throughputs of hydrogen processing facilities are constrained by their minimum and maximum capacity limits, which are represented by the following equations:

$$Pcapmin_p \cdot NP_p \leq Pr_p \leq Pcapmax_p \cdot NP_p \quad (15)$$

$$Ccapmin_c \cdot NC_c \leq Cr_c \leq Ccapmax_c \cdot NC_c \quad (16)$$

$$S_1capmin_{s_1} \cdot NS1_{s_1} \leq S_1Inv_{s_1} \leq S_1capmax_{s_1} \cdot NS1_{s_1} \quad (17)$$

$$Rcapmin_r \cdot NR_r \leq Rr_r \leq Rcapmax_r \cdot NR_r \quad (18)$$

where  $Pcapmin_p$ ,  $Ccapmin_c$ ,  $S_1capmin_{s_1}$ , and  $Rcapmin_r$  are the minimum capacities of hydrogen production ( $p$ ), conditioning ( $c$ ), storage ( $s$ ), and reconversion ( $r$ ), respectively.  $Pcapmax_p$ ,  $Ccapmax_c$ ,  $S_1capmax_{s_1}$ , and  $Rcapmax_r$  are the maximum capacities of hydrogen production ( $p$ ), conditioning ( $c$ ), storage ( $s$ ), and reconversion ( $r$ ), respectively.

In addition to the aforementioned constraints, the connectivity of the superstructure network, energy source availability, transportation circumstances at the demand site, and the required storage inventory level are also considered as constraints.

## 5. CASE STUDY

To demonstrate the functionality of this framework, a case study is conducted with the production site in Saudi Arabia and the demand site in Texas. In this context, the hydrogen supplier is situated in Saudi Arabia, and conditioned hydrogen is transported to the Port of Houston, serving as the national distribution center. Moreover, Houston, Dallas, Fort Worth, San Antonio, and Austin in Texas house most of the state's population, with RDCs strategically positioned in these cities. Additionally, LDCs, corresponding to intracity refueling stations in urban areas, are located within each city as per the Idealized Refueling Station Network Model.

### 5.1 Hydrogen demand estimation

The hydrogen demand projection in Texas is calculated based on the market share of fuel cell electrical vehicles (FCEV), the number of enrolled cars in Texas, average travel distance of a driver in Texas, and the fuel economy of FCEV as shown below:

$$HD = MS \cdot N^{car} \cdot AvD \cdot FE^{car} \quad (19)$$

where  $MS$  is the market share of hydrogen FCEV,  $N^{car}$  is the number of cars in Texas,  $AvD$  is the average travelled distance of a driver in Texas, and  $FE^{car}$  is the fuel economy of FCEV.

### 5.2 The optimal hydrogen supply chain configuration

Considering the developed superstructure and formulated optimization problem, the optimal hydrogen pathway is identified at a 30% of market share. The most cost-effective hydrogen supply path begins with steam methane reforming using natural gas. The hydrogen is then converted to ammonia and delivered sequentially from the NDC to the LDC via an ammonia trailer. Finally, the ammonia is reconverted into hydrogen for delivery to the end customer. The cost hierarchy derived from this superstructure optimization is Ammonia, Liquid hydrogen (LH<sub>2</sub>), LOHC, and Compressed gas hydrogen (GH<sub>2</sub>).

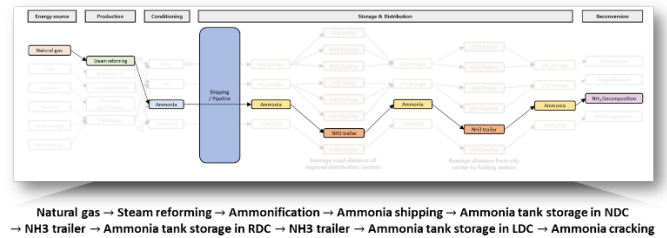


Figure 5. Cost-efficient configuration of a hydrogen supply chain

### 5.3 Levelized cost of hydrogen from the optimal configuration

The breakdown of costs for a 30% market share is illustrated in Fig. 6. Among the overall expenses of the HSC, ammonification emerges as the most substantial component in terms of total cost. Despite the comparatively high conditioning and reconversion costs associated with ammonia when compared to alternative options, it was selected as the optimal route. This decision stems from the considerable cost savings realized during hydrogen transportation facilitated by ammonia's high volumetric energy density.

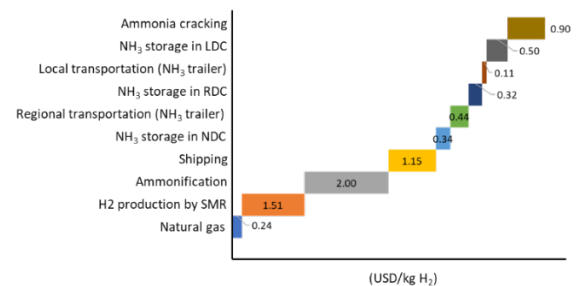


Figure 6. H<sub>2</sub> levelized cost from the optimal pathway

### 5.4 Sensitivity analysis according to market penetration rate.

Fig. 7 depicts the total cost under a fixed maximum capacity for each transportation mode based on market share. Generally, an increase in market share is associated with a decrease in prices. However, when operating under a fixed maximum infrastructure capacity, if the hydrogen demand surpasses the maximum capacity of the optimal route, additional hydrogen is drawn from suboptimal routes. This dynamic leads to a

gradual increase in prices with an increase in market share. As a prospective avenue for future research, a multi-period optimization study can be proposed to determine the feasibility of incrementally enhancing each infrastructure's capacity over time.

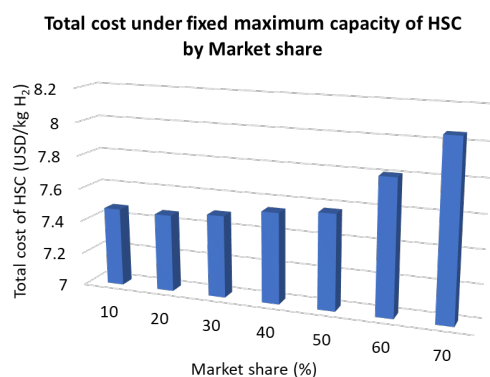


Figure 7. Total cost of hydrogen supply chain by market share

## 6. CONCLUSIONS

In this study, a comprehensive framework of the entire HSC is developed with a particular emphasis on incorporating both conventional and promising technologies in the established superstructure. The regional and local transportation systems are elucidated using GIS data and the Idealized Refueling Station Network Model, respectively. The inclusion of promising early-stage technologies is supported by data generated through process modeling and simulation techniques. Notably, the CO<sub>2</sub> hydrogenation to formic acid process is simulated and rigorously evaluated through techno-economic analysis. The identification of a cost-efficient HSC configuration marks a significant contribution, demonstrating the practical applicability of the developed framework. The realism of the study is further enhanced through a detailed case study involving the production site in Saudi Arabia and the demand site in Texas. The optimal hydrogen pathway is determined via MILP optimization applied to the developed HSC superstructure network. Looking ahead, a future avenue involves conducting multi-objective optimization that considers both cost and CO<sub>2</sub> emissions simultaneously. The approach aims to offer a holistic perspective on optimal configurations that align with both economic and environmental objectives.

## REFERENCES

Agnolucci, P., & McDowall, W. (2013). Designing future hydrogen infrastructure: Insights from analysis at different spatial scales. *International Journal of Hydrogen Energy*, 38(13), 5181–5191.

Almansoori, A., & Shah, N. (2006). Design and Operation of a Future Hydrogen Supply Chain: Snapshot Model. *Chemical Engineering Research and Design*, 84(6), 423–438.

Endo, E. (2007). Market penetration analysis of fuel cell vehicles in Japan by using the energy system model MARKAL. *International Journal of Hydrogen Energy*, 32(10), 1347–1354.

Eskandarpour, M., Dejax, P., Miemczyk, J., & Péton, O. (2015). Sustainable supply chain network design: An optimization-oriented review. *Omega*, 54, 11–32.

Gül, T., Kyreos, S., Turton, H., & Barreto, L. (2009). An energy-economic scenario analysis of alternative fuels for personal transport using the Global Multi-regional MARKAL model (GMM). *Energy*, 34(10), 1423–1437.

Hurskainen, M., & Itonen, J. (2020). Techno-economic feasibility of road transport of hydrogen using liquid organic hydrogen carriers. *International Journal of Hydrogen Energy*, 45(56), 32098–32112.

Kalamaras, C. M., & Efstathiou, A. M. (2013). Hydrogen Production Technologies: Current State and Future Developments. *Conference Papers in Energy*, 2013, 690627.

Kuby, M., & Lim, S. (2005). The flow-refueling location problem for alternative-fuel vehicles. *Socio-Economic Planning Sciences*, 39(2), 125–145.

Kuby, M., Lines, L., Schultz, R., Xie, Z., Kim, J.-G., & Lim, S. (2009). Optimization of hydrogen stations in Florida using the Flow-Refueling Location Model. *International Journal of Hydrogen Energy*, 34(15), 6045–6064.

Lin, Z., Ogden, J., Fan, Y., & Chen, C.-W. (2008). The fuel-travel-back approach to hydrogen station siting. *International Journal of Hydrogen Energy*, 33(12), 3096–3101.

Nicoletti, G., Arcuri, N., Nicoletti, G., & Bruno, R. (2015). A technical and environmental comparison between hydrogen and some fossil fuels. *Energy Conversion and Management*, 89, 205–213.

Noh, H., Kang, K., & Seo, Y. (2023). Environmental and energy efficiency assessments of offshore hydrogen supply chains utilizing compressed gaseous hydrogen, liquefied hydrogen, liquid organic hydrogen carriers and ammonia. *International Journal of Hydrogen Energy*, 48(20), 7515–7532.

Rosenberg, E., Fidje, A., Espegren, K. A., Stiller, C., Svensson, A. M., & Møller-Holst, S. (2010). Market penetration analysis of hydrogen vehicles in Norwegian passenger transport towards 2050. *International Journal of Hydrogen Energy*, 35(14), 7267–7279.

Strachan, N., Balta-Ozkan, N., Joffe, D., McGeevor, K., & Hughes, N. (2009). Soft-linking energy systems and GIS models to investigate spatial hydrogen infrastructure development in a low-carbon UK energy system. *International Journal of Hydrogen Energy*, 34(2), 642–657.

Tsuda, K., Kimura, S., Takaki, T., Toyofuku, Y., Adaniya, K., Shinto, K., Miyoshi, K., Hirata, K., Christiani, L., Takada, M., Kobayashi, N., Baba, S., Nagamatsu, Y., & Takata, M. (2014). Design proposal for hydrogen refueling infrastructure deployment in the Northeastern United States. *International Journal of Hydrogen Energy*, 39(14), 7449–7459.

Yang, C., & Ogden, J. (2007). Determining the lowest-cost hydrogen delivery mode. *International Journal of Hydrogen Energy*, 32(2), 268–286.